Chemosphere 125 (2015) 130–138

Contents lists available at ScienceDirect

Chemosphere

journal homepage: www.elsevier.com/locate/chemosphere

Removal of colloidal biogenic selenium from wastewater

Lucian C. Staicu [a,b], Eric D. van Hullebusch [b,*], Mehmet A. Oturan [b], Christopher J. Ackerson [c], Piet N.L. Lens [a]

[a] UNESCO-IHE Institute for Water Education, PO Box 3015, 2601 DA Delft, The Netherlands
[b] Université Paris-Est, Laboratoire Géomatériaux et Environnement, EA 4508, UPEM, 5 bd Descartes, 77454 Marne-la-Vallée Cedex 2, France
[c] Department of Chemistry, Colorado State University, Fort Collins, CO 80521, United States

HIGHLIGHTS

- Colloidal stability of Se(0) is linked to its nanosize and ζ-potential (−20 ± 5 mV).
- High speed (4500 rpm) centrifugation achieved 91% Se(0) removal.
- Filtration through 0.45 μm filters yields a Se(0) removal efficiency of 87%.
- Aluminum sulfate (10^{-3} M) can sediment up to 92% of colloidal elemental selenium.
- Al–Se sediment shows better dewaterability than Fe–Se sediment.

GRAPHICAL ABSTRACT

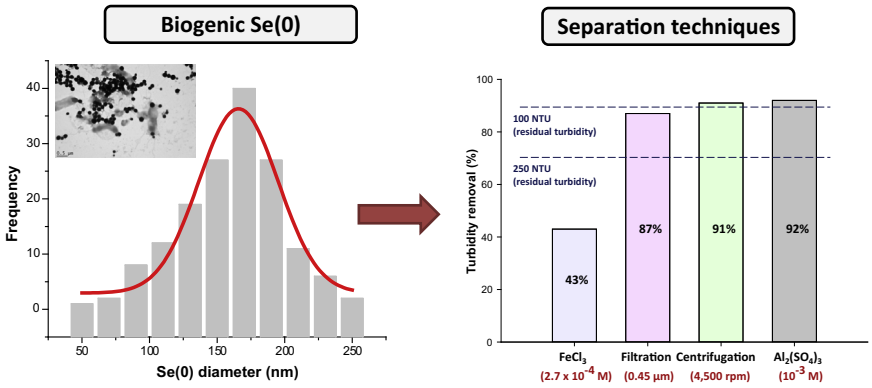

ARTICLE INFO

Article history:
Received 25 August 2014
Received in revised form 5 November 2014
Accepted 1 December 2014
Available online 3 January 2015

Handling Editor: Min Jang

Keywords:
Elemental selenium
Colloids
Coagulation–flocculation
Aluminum sulfate
Filtration
Centrifugation

ABSTRACT

Biogenic selenium, Se(0), has colloidal properties and thus poses solid–liquid separation problems, such as poor settling and membrane fouling. The separation of Se(0) from the bulk liquid was assessed by centrifugation, filtration, and coagulation–flocculation. Se(0) particles produced by an anaerobic granular sludge are normally distributed, ranging from 50 nm to 250 nm, with an average size of 166 ± 29 nm and a polydispersity index of 0.18. Due to its nanosize range and protein coating-associated negative zeta potential (−15 mV to −23 mV) between pH 2 and 12, biogenic Se(0) exhibits colloidal properties, hampering its removal from suspension. Centrifugation at different centrifugal speeds achieved 22 ± 3% (1500 rpm), 73 ± 2% (3000 rpm) and 91 ± 2% (4500 rpm) removal. Separation by filtration through 0.45 μm filters resulted in 87 ± 1% Se(0) removal. Ferric chloride and aluminum sulfate were used as coagulants in coagulation–flocculation experiments. Aluminum sulfate achieved the highest turbidity removal (92 ± 2%) at a dose of 10^{-3} M, whereas ferric chloride achieved a maximum turbidity removal efficiency of only 43 ± 4% at 2.7×10^{-4} M. Charge repression plays a minor role in particle neutralization. The sediment volume resulting from $Al_2(SO_3)_4$ treatment is three times larger than that produced by $FeCl_3$.

1. Introduction

Selenium (Se) is a chalcogen element sharing common properties with sulfur (S) and tellurium (Te). Se has a complex

* Corresponding author. Tel.: +33 1 49 32 90 42; fax: +33 1 49 32 91 37.
E-mail address: Eric.vanHullebusch@u-pem.fr (E.D. van Hullebusch).

http://dx.doi.org/10.1016/j.chemosphere.2014.12.018
0045-6535/

biogeochemistry and is circulated through environmental compartments via both natural and anthropogenic processes (Chapman et al., 2010). Natural sources of selenium are crustal weathering and leaching, volcanism, sea salt spraying, and biological activities (Wen and Carignan, 2007). The anthropogenic release of selenium in the environment is mainly related to fossil fuel combustion, mining, non-metal smelting, and agriculture practiced on seleniferous soils (Lemly, 2004).

Of special interest is the very narrow window between selenium essentiality and toxicity (Levander and Burk, 2006). Based on blood plasma glutathione peroxidase activity as the selenium biomarker, a dietary reference intake (DRI) of 55 $\mu g\, d^{-1}$ is proposed (IOM, 2000). In excess, selenium poisoning (i.e. selenosis) can result in hair loss, brittle nails and neurological pathologies (e.g. decreased cognitive function, convulsions, and weakness) (Tinggi, 2003). Estimated maximal intake levels of 910 $\mu g\, Se\, d^{-1}$ caused by agriculture practiced on seleniferous soils were linked to endemic selenosis in China (Yang et al., 1989). The toxicity elicited by Se on biota is mainly related to the chemical speciation that selenium undergoes under changing redox conditions. Amongst its oxidation states, Se oxyanions, namely selenite (Se[IV], SeO_3^{2-}) and selenate (Se[VI], SeO_4^{2-}), are water-soluble, bioavailable and toxic (Simmons and Wallschlaeger, 2005). In contrast, elemental selenium, Se(0), is solid and less toxic (Dungan and Frankenberger, 1999). Nevertheless selenium nanoparticles (SeNPs) exhibited significant toxicity to mice (Zhang et al., 2005). In addition, particulate Se(0) has been reported to be bioavailable to bivalves (Luoma et al., 1992; Schlekat et al., 2000) and fish (Li et al., 2008). Furthermore, Se(0) is prone to re-oxidation to toxic SeO_3^{2-} and SeO_4^{2-} when discharged into aquatic ecosystems (Zhang et al., 2004).

A number of treatment technologies, including biological methods, aim to remove selenium oxyanions present in industrial wastewaters by reducing them to solid-phase elemental selenium (Lenz and Lens, 2009; Sobolewski, 2013). When biological treatment of selenium-laden wastewaters is performed, biogenic Se(0) is the solid end product that can be removed from the aqueous phase (Staicu et al., 2014). Due to its surface charge and nanometer size, biogenic Se(0) exhibits colloidal stability making its removal from the water phase difficult (Buchs et al., 2013). Coagulation–flocculation is one of the main processes employed both in drinking and wastewater treatment for the removal of colloidal and suspended particles (Duan and Gregory, 2003). The principle relies on the destabilization and settling of the colloids and suspended particles that cannot settle by gravity within practical time frames. Because of their proven efficiency and low cost, aluminum sulfate and ferric chloride are currently employed as coagulants on a large scale (Gregory and Duan, 2001). When coagulants are added to water, the metal ions (e.g. Al^{3+}, Fe^{3+}) hydrolyze spontaneously and form a series of metastable metal hydrolysis products (Richens, 1997). These metal hydrolysis products act upon the negatively charged particles held in suspension by hydrostatic repulsion forces (Russel et al., 1992). They alter the physical state of the suspended particles by repressing their charge (i.e. charge repression) and by forming large aggregates of $Al(OH)_3$/$Fe(OH)_3$ (i.e. sweep flocculation) which lead to particle sedimentation (Gregory and Duan, 2001). The use of filtration has been reported for removing colloidal particles other than Se(0). In a recent study, Johnson et al. (2014) has investigated the removal of particulate and colloidal silver in the sewage effluent discharged from several British wastewater treatment plants. On the other hand, centrifugation is rarely used for removing colloidal particles because it is an energy intensive process, but this approach can become feasible when treating highly turbid wastewaters (Thuvander et al., 2014).

Regardless of the utilization of coagulation–flocculation on a large scale for the removal of colloidal particles (Duan and Gregory, 2003), no systematic study has been done to investigate the separation of biologically-produced colloidal Se(0) from the bulk solution. The objectives of this study were, therefore, to characterize surface charge, stability and particle size distribution of biogenic Se(0) particles and to assess the solid–liquid separation potential of colloidal elemental selenium by filtration, centrifugation and coagulation–flocculation.

2. Materials and methods

2.1. Chemicals and media

Sodium selenate, Na_2SeO_4, ⩾98.0%, was purchased from Sigma Aldrich and fresh solutions were prepared before each experiment. All other reagents were of analytical grade. Ferric chloride hexahydrate, $FeCl_3{\cdot}6H_2O$ (ACS reagent, >98%) and aluminum sulfate octadecahydrate, $Al_2(SO_4)_3{\cdot}18H_2O$ (ACS grade, >98%) were purchased from Sigma Aldrich and Fischer Scientific, respectively. All solutions were prepared using deionized water.

Incubations were done using Basal Mineral Medium (BMM) containing ($g\, L^{-1}$): NH_4Cl (0.3), NaCl (0.3), $CaCl_2.2H_2O$ (0.11), $MgCl_2.6H_2O$ (0.1), 1 $mL\, L^{-1}$ acid trace element solution, 1 $mL\, L^{-1}$ basic element solution, and 0.2 $mg\, L^{-1}$ of vitamin solution (Stams et al., 1993). 10 mM sodium selenate and 20 mM lactate (as sodium L-lactate) were amended to the BMM.

2.2. Production of biogenic red Se(0)

BMM containing sodium selenite and 15 $g\, L^{-1}$ (wet weight) inoculum was transferred to serum bottles. Anaerobic granular sludge sampled from an Upflow Anaerobic Sludge Blanket (UASB) reactor treating brewery wastewater was used as inoculum. The sludge was kindly provided by Biothane Systems International (Delft, the Netherlands) and the same sludge was used throughout all experiments. The inoculum had a Total Suspended Solids (TSS) and a Volatile Suspended Solids (VSS) content of, respectively, 54.6 $g\, L^{-1}$ and 39.8 $g\, L^{-1}$, corresponding to a VSS/TSS ratio of 0.73 (Kijjanapanich et al., 2013).

The bottles were closed with butyl rubber septa and aluminum caps, the headspace was flushed with nitrogen gas for 15 min and the final headspace pressure adjusted to 1.7 bar (Astratinei et al., 2006). Incubation was performed at 30 °C, in the dark and under constant shaking at 100 rpm for 14 d.

At the end of the incubation period, the colorless Na_2SeO_4 solution had developed a red color (Fig. 1a), indicative of biogenic Se(0) formation (Oremland et al., 2004). The Se(0) particles produced through microbial reduction of selenium oxyanions are designated 'biogenic' and represent the red allotrope of elemental selenium (Fellowes et al., 2011). After 14 d of incubation, bottles containing red Se(0) were left in a vertical position for 6 h allowing for the separation of the granular sludge inoculum from the bulk Se(0) solution. Se(0)-containing supernatant was carefully transferred to new recipients and used for coagulation experiments.

2.3. Se(0) protein-coating characterization

After sampling biogenic Se(0), the red suspension was centrifuged at 10 000*g* for 5 min and the pellet was washed three times in sterile Phosphate Buffer Saline (PBS). The proteins that were attached onto the biogenic Se(0) particles were denatured by the addition of 160 mM dithiothreitol (DTT) and 1% SDS (Sodium Dodecyl Sulfate) followed by boiling the samples at 95 °C in a water bath for 5 min. The denatured samples (60 µL) were loaded into 15% denaturing gels and run at constant current (30 mA) for 2 h in TBE (1×) buffer using Polyacrylamide Gel Electrophoresis

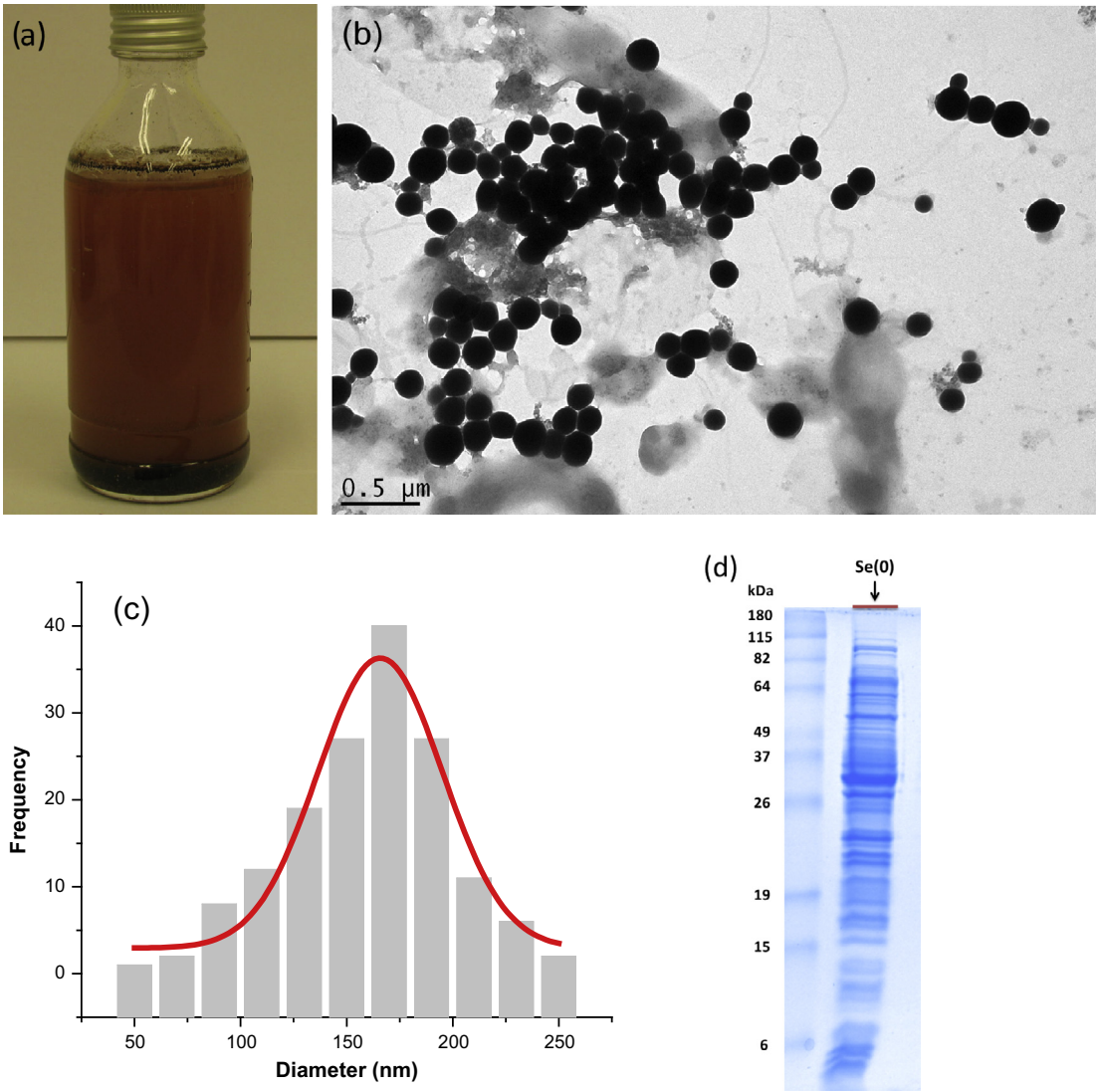

Fig. 1. (a) Biogenic red Se(0) produced by anaerobic granular sludge inoculum (incubation at: 30 °C, pH 7.5, anaerobic, dark, 100 rpm), (b) transmission electron micrograph of biogenic red Se(0) produced by anaerobic granular sludge (same incubation conditions as (a)), (c) size distribution of biogenic Se(0) particles. Note: $n = 155$, $R^2 = 0.93$, $\sigma < 5\%$, (d) SDS–PAGE gel image (Coomassie Blue G-420 stain) of proteins associated with biogenic Se(0) (right lane) and molecular standards in kilodaltons (left lane). Note that the arrow shows the red Se(0) that remained in the well after the gel was run. (For interpretation of the references to color in this figure legend, the reader is referred to the web version of this article.)

(SDS–PAGE) (Laemmli, 1970). Coomassie™ Blue G-250 (limit of detection [LOD], 25 ng/band) was used to stain the protein bands.

2.4. Jar-test experiments

Coagulation tests were conducted in triplicate at room temperature (21 °C) using a Velp Scientifica 6 places flocculator (JLT6) in standard 500 mL glass beakers (88 mm internal diameter × 122 mm height) containing 300 mL of Se(0) suspension. The 25 mm high × 75 mm wide × 1 mm thick stirring paddles were immersed roughly at the middle height of the sample. The coagulation protocol followed the standard coagulation stages (adapted from USEPA, 1999): *rapid mixing* at 90 rpm (which corresponds to a mean velocity gradient, $G = 55.7\ s^{-1}$) for 1 min, *slow mixing* (floc formation) at 20 rpm ($G = 6.8\ s^{-1}$) for 25 min and *sedimentation* (no stirring) in graduated Imhoff cones for 60 min.

Ferric chloride and aluminum sulfate were employed for the chemical coagulation study (Fig. 4a). The coagulant concentration employed ranged from 0 (controls) to 10^{-3} M. This range was chosen based on previous studies on colloidal particle removal from humic substances, dissolved organic matter, kaolin model solutions and combined sewer overflow by coagulation–flocculation (Jung et al., 2005; Canizares et al., 2007; El Samrani et al., 2008).

Experiments were initiated by adding 10 mL of different concentrations of both coagulants (ferric chloride and aluminum sulfate) under agitation to every sample at a point below the free surface of the liquid (El Samrani et al., 2008). After 60 min of sedimentation, the sediment volume was read and 100 mL of supernatant was transferred to polyethylene sampling cups. Residual turbidity, conductivity, pH, and electrophoretic mobility measurements were performed shortly after. The sediment was recovered for further measurements, after the remaining supernatant was carefully siphoned with a glass pipette.

The following controls were included: (1) sterile treatments containing BMM and selenate without inoculum to assess the abiotic selenate conversion, (2) treatments containing BMM and inoculum to assess the turbidity produced by suspended microbial growth, (3) Se(0) treatments without coagulant to assess gravitational sedimentation of the Se(0) particles.

Centrifugation of the biogenic Se(0) particles was performed using a Rotina 420 centrifuge with a 4784-A rotor accommodating 15 mL tubes at three centrifugal speeds: 1500 rpm (≈463*g*), 3000 rpm (≈1851*g*), and 4500 rpm (≈4166*g*). Filtration of the biogenic Se(0) particles was done using 0.45 μm (poly)tetrafluoroethylene (PTFE) syringe filters.

2.5. Analysis

Turbidity (Hach DR/890 Colorimeter) and pH (Metrohm 691 and a SenTix 21 WTW pH electrode) were measured at the beginning and at the end of the Jar-Test experiments. Turbidity was expressed in Nephelometric Turbidity Units (NTU) and measured according to USEPA (1999). The volume of settled Se(0) was measured in standard 1000 mL Imhoff graduated cones (USEPA, 1999). Conductivity measurements were performed on a Radiometer Analytical MeterLab CDM 230.

Electrophoretic mobility measurements were performed on a Zetasizer Nano ZS (Malvern Instrument Ltd., Worchestershire, UK) using a laser beam at 633 nm and a scattering angle of 173° at 25 °C according to the manufacturer's instructions. The impact of pH on the Se(0) particle surface charge was investigated using an MPT-2 autotitrator upgraded to the Zetasizer Nano ZS.

For Transmission Electron Microscopy (TEM), samples were loaded into dialysis tubing (Fisher, 25 μm wall thickness, molecular weight cutoff = 3500 Da) and dialyzed against 20 mM Tris solution (pH 7.4). The buffer was exchanged three times at three-hour intervals. 5 μL of a dialyzed sample were pipetted onto 400 mesh carbon coated copper TEM grids (EM Sciences). The resulting samples were examined in a JEOL JEM-1400 TEM operated at 100 kV and spot size 1. The Se(0) particle size distribution was determined by TEM image processing using ImageJ™ 1.47v software.

Capillary Suction Time (CST) was measured at room temperature with a Triton Model 200 CST Apparatus as described in the Instruction Manual and reported by Scholz (2005) using 5 mL of Se(0) suspension. Whatman no. 17 blotting paper was used in all CST measurements (Scholz, 2006).

2.6. Data analysis

All data were analyzed by using the data analysis software SigmaPlot 12.0v. The results are presented as average values and standard deviation (σ) of three independent experiments (triplicates, $n = 3$) unless otherwise stated. When the standard deviation values were smaller than 5%, the error bars were not represented. The Polydispersity Index (PDI) of Se(0) particles was calculated by dividing the standard deviation by the mean diameter of the particles.

3. Results

3.1. Biogenic Se(0) particle characterization

A representative TEM micrograph of red biogenic Se(0) solution (Fig. 1a) is presented in Fig. 1b. Biogenic elemental selenium consists of round-shaped and polydispersed particles (Fig. 1b and c). The characteristics of Se(0) particles are compiled in Table 1, showing that the surface charge of the Se(0) particles exhibited a negative zeta potential value at neutral pH. Fig. 1d presents the protein bands that were attached to the biogenic Se(0) particles. Based on the protein ladder used as a reference, the bands were characterized by molecular weights (in kDa) in the 115 to below 6 kDa range.

Fig. 2 presents the biogenic Se(0) surface charge variation as a function of pH. In order to assess the influence of pH on the surface charge of Se(0) particles, the pH change was performed in both the acidic and basic domains starting from the initial pH of 7.7. Adding HCl or NaOH to a solution increases its ionic strength, which in turn acts by repressing the hydrodynamic diameter of the particles. When the pH of the Se(0) containing solution was increased, the initial zeta potential value (−23 mV, pH 7.7) also increased, reaching the highest value of −16.7 mV at pH 9.5. Above pH 9.5, the surface charge of Se(0) particles leveled off with a final zeta potential value of −17 mV at pH 12.5. Conversely, when the solution was acidified, the Se(0) particles displayed a higher increase in their surface charge reaching −13.8 mV at pH 2.6.

Table 2 summarizes the characteristics of the Se(0) solution. The solution is characterized by high turbidity, deep red color (Fig. 1a) and neutral pH. In contrast, the treatments without sodium selenate in the medium generated a turbidity below 5 NTU after 14 d of incubation under similar conditions. Therefore, the high solution turbidity (≈850 NTU) recorded for the incubations containing sodium selenate can be attributed to the red Se(0) observed both visually (Fig. 1a) and with TEM (Fig. 1b).

Fig. 3a shows the control treatment of Se(0) settling by gravitation over the time course of 4 d. The results are presented as normalized (C/C_0) colloidal stability where C represents the turbidity

Table 1
Characteristics of biogenic red Se(0) particles (incubated at 30 °C, initial pH, $pH_0 = 7.5$, anaerobic, dark, 100 rpm).

Parameter	Value
Shape	Spherical
Size range (nm)	50–250
Mean size (nm)	166 ± 29
Polydispersity index	0.18
Zeta potential (mV)[a]	−23 ± 3
Isoelectric point	Not reached

[a] Measured at pH 7.7.

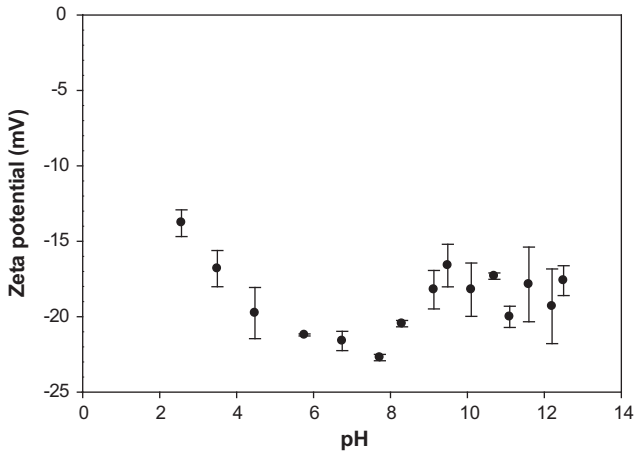

Fig. 2. Variation of the zeta potential of biogenic Se(0) as a function of pH. Note that titration started at pH 7.7 and proceeded toward low and high pH.

Table 2
Properties of biogenic Se(0) solution (produced at 30 °C, $pH_0 = 7.5$, anaerobic, dark, 100 rpm).

Parameter	Value
Turbidity (NTU)	850 ± 50
Color	Red
pH	7.5 ± 0.3
Conductivity (mS cm^{-1})	4.8 ± 0.2

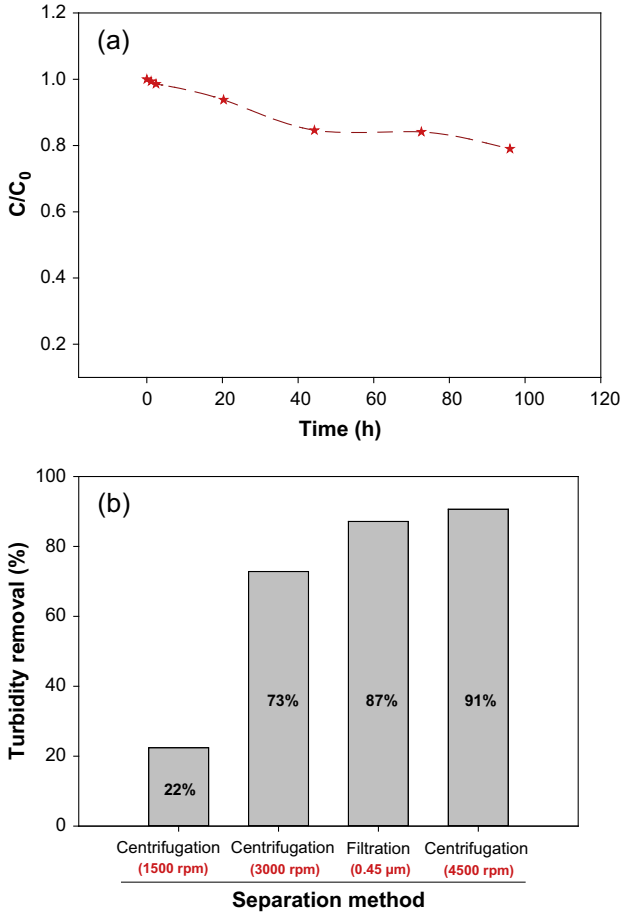

Fig. 3. (a) Biogenic Se(0) gravitational settling (C – turbidity at time t, C_0 – initial turbidity), and (b) removal of biogenic Se(0) using filtration and centrifugation at different speed values.

measured at different time points and C_0 is the initial turbidity. After a period of 4 d, biogenic Se(0) stored in Imhoff sedimentation cones exhibited only limited settling, 0.8 out of 1 (initial normalized turbidity), which corresponds to 179 NTU less turbidity.

3.2. Turbidity removal

Fig. 3b depicts the Se(0) removal efficiency using centrifugation. The removal efficiency increased with centrifugal force: 1500 rpm removed 22 ± 3% of colloidal Se(0), 3000 rpm achieved 73 ± 2% and 4500 rpm reached a Se(0) removal efficiency of 91 ± 2%. Filtration on a 0.45 μm cut-off filter removed 87 ± 1% of the initial Se(0).

The addition of aluminum sulfate improved the turbidity removal as a function of coagulant concentration added (Fig. 4a). The lowest concentrations of coagulants (0.1–1.3 × 10^{-4} M) were not strong enough to impact the colloidal stability of biogenic Se(0) particles. When dosing 1.3–2.7 × 10^{-4} M aluminum sulfate, turbidity removal exhibited a marked increase from 2% to 57%, indicative of a threshold value that triggers the massive particle destabilization. Above 2.7 × 10^{-4} M, the decrease in turbidity was less pronounced until it reached about 92% removal efficiency for the highest coagulant dose used, 10^{-3} M.

In contrast to aluminum sulfate, ferric chloride displayed a different turbidity removal curve and efficiency (Fig. 4a). While it reached the threshold point (0.7 × 10^{-4} M) and the breakthrough domain of the curve faster than aluminum sulfate, the maximum removal efficiency achieved was only 43% for 4 × 10^{-4} M. Beyond this point, the removal efficiency undergoes a slow decline reaching 33% for 10^{-3} M. In terms of residual turbidity (Fig. 4a and Table 2), the lowest value (70 NTU), was obtained for 10^{-3} M aluminum sulfate. Comparatively, the addition of ferric chloride could not decrease the turbidity below 458 NTU.

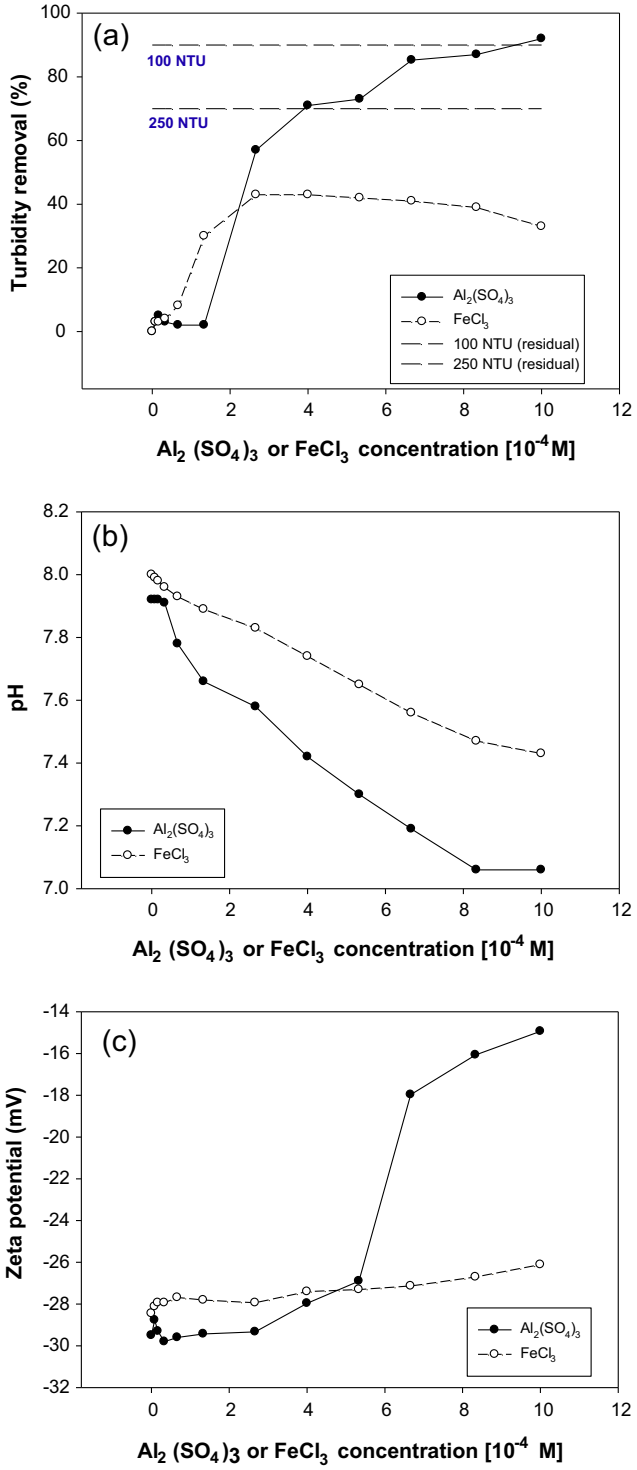

Fig. 4. (a) Evolution of the Se(0) removal efficiency with coagulant dose. Note that 250 NTU and 100 NTU dashed lines indicate residual turbidity, (b) pH change of Se(0) solution as a function of coagulant dosage, and (c) evolution of zeta potential with aluminum sulfate and ferric chloride concentration.

Fig. 4b shows the change in pH over the coagulant dose range. Both treatments displayed decreasing pH with coagulant concentration, but the decrease was within one pH unit (from 8 to 7).

Aluminum sulfate addition showed a more pronounced pH drop than ferric chloride.

3.3. Se(0) surface charge

Fig. 4c shows the evolution of biogenic Se(0) surface charge as a function of coagulant concentration. In the case of aluminum sulfate addition, the zeta potential decreased from −30 mV (control) to −15 mV (10^{-3} M), whereas iron chloride dosing was accompanied by a minor zeta potential change, from −28 mV (control) to −26 mV (for a concentration of 10^{-3} M).

3.4. Characterization of sediment

To clarify the effect of coagulant dosing on the sediment volume, measurements of sediment volume for each treatment were performed. Fig. 5a presents the sediment volume resulting from the interaction between aluminum sulfate or ferric chloride and biogenic elemental selenium. In the case of aluminum sulfate, the sediment volume increased steadily reaching a maximum volume of 26 mL for the highest coagulant dose applied. In contrast, ferric chloride produced less sediment, showing a smooth increase until a maximum value of 8 mL for 10^{-3} M coagulant. For both coagulants, the first doses induced limited sedimentation. The sediment volume resulting from $Al_2(SO_3)_4$ treatment is about three times higher than that produced by $FeCl_3$.

Fig. 5b presents the CST profile of the sediment collected during aluminum sulfate and ferric chloride treatment. For $Al_2(SO_4)_3$ treatment, the CST decreased with increasing coagulant dose, from 120 s to 87 s. The $FeCl_3$ treatment induced a reversed trend: the CST was increasing with coagulant dose from 86 s to 127 s.

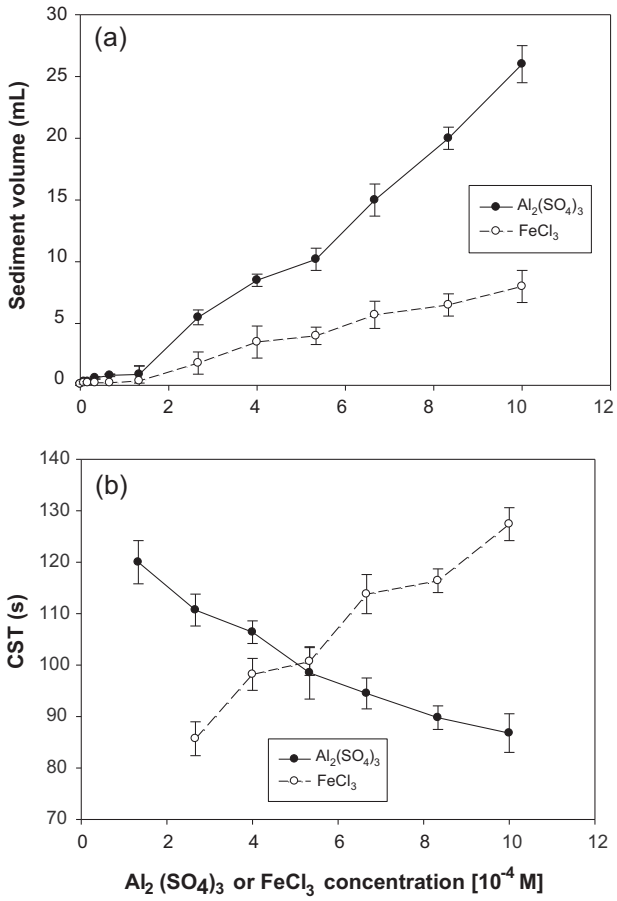

Fig. 5. (a) Effect of coagulant dose on sediment volume, (b) evolution of CST of Al–Se and Fe–Se sediments as a function of coagulant concentration.

4. Discussion

4.1. Turbidity removal

This study showed that aluminum sulfate is an effective coagulating agent to destabilize and sediment colloidal biogenic Se(0). In contrast, ferric chloride achieved only limited Se(0) removal. This difference might be related to the hydrolysis products of iron and aluminum obtained as a function of pH, which are significantly different. Even if both metals exhibit 4 deprotonations, from aquo Fe^{3+}/Al^{3+} complexes to $Fe(OH)_4^-$/$Al(OH)_4^-$, aluminum hydrolysis species occur cooperatively and cover a much narrower pH range compared to iron species (Martin, 1991). This is explained by the transition from octahedral hexahydrate $Al^{3+}{\cdot}6H_2O$ to tetrahedral $Al(OH)_4^-$, while in the case of iron its hydrolyzed species retain the octahedral co-ordination even if they span around 8 pH units (Martin, 1991). Apart from the mononuclear hydrolysis products, polymeric species can also play a role, although they are present in low concentrations and are inhibited by organic molecules (Duan and Gregory, 2003).

Flocculation is the second stage in chemical coagulation and has been shown to greatly impact the treatment effectiveness (Jarvis et al., 2005). Flocs are composed of a complex arrangement of solid particles, hydroxide precipitates and water entrapped during flocculation (Hogg, 2005). Floc growth is characterized by several phases until reaching a steady state between aggregation and fragmentation (Tambo, 1991). Ferric flocs were shown to be smaller and less compact than their aluminum sulfate counterparts, entailing also a poorer settleability (Turchiuli and Fargues, 2004). Ferric chloride displayed an Optimal Coagulant Concentration (OCC), defined as the coagulant dose that achieves the highest turbidity removal at 4×10^{-4} M, whereas the aluminum sulfate treatment did now show an OCC within the coagulant range investigated.

Prior to coagulation–flocculation, centrifugation was assessed as a potential solid–liquid separation method. The highest removal efficiency (91%) of Se(0) was achieved through high-speed centrifugation at 4500 rpm. Filtration through 0.45 μm cut-off filters ranked second with 87% efficiency (Fig. 3b). Although its removal efficiency was close to the performance of aluminum sulfate treatment, centrifugation cannot be employed on a full-scale situation due to prohibitive costs related to energy consumption and other capital and operating expenses. Additionally, pretreatment, membrane fouling and the need for further treatment of the retentate are serious drawbacks. In a companion article (Staicu et al., 2014), electrocoagulation using Al and Fe sacrificial electrodes was employed to sediment colloidal Se(0) produced by a strain of *Pseudomonas moraviensis*. The best Se(0) turbidity removal (97%) was achieved using iron electrodes at 200 mA. Aluminum electrodes removed 96% of colloidal Se(0) only at a higher current intensity (300 mA). While more efficient, electrocoagulation involves the use of electricity and metallic electrodes that are being consumed progressively. An interesting complementary approach to coagulation–flocculation or electrocoagulation might be the use of mesoporous silica conjugate adsorbents, that have been shown to selectively detect and remove residual Se-oxyanions from aqueous media (Awual et al., 2014).

4.2. Se(0) charge repression

A number of coagulation mechanisms have been proposed dependent on the pollutant and physical–chemical properties of the solution and coagulant dosed (Duan and Gregory, 2003). These

mechanisms include charge neutralization, bridging, sweep flocculation and double layer compression (Holt et al., 2002). In order to assess the mechanism involved in the biogenic Se(0) sedimentation, zeta potential measurements were performed for all applied coagulant doses and for the control treatments. Fig. 4c shows that both coagulants act by repressing the surface charge (zeta potential) of Se(0) particles, but not up to the point of zero charge (PZC). This set of data indicates that charge repression contributes to the coagulation process to a lesser extent. Consequently, other coagulation mechanisms like sweep flocculation or adsorption appear to play the major role in the overall Se(0) removal by coagulant addition. However, the fact that both aluminum sulfate and ferric chloride acted by decreasing the surface charge of Se(0) particles should not be overlooked. Coagulation–flocculation is a complex phenomenon wherein several mechanisms are involved (Duan and Gregory, 2003). Similar results within the same pH range were reported for humic acid and kaolin suspensions (Zhao et al., 2011). Charge repression has been reported to act preferentially at acidic pH, whereas sweep flocculation and adsorption apply at neutral pH where abundant metal hydroxide precipitation is encountered (Edwards and Amirtharajah, 1985).

The change in pH (Fig. 2) cannot repress the surface charge of Se(0) particles to the point of rendering them neutral. A possible explanation can be the protein layers that are coating biogenic Se(0) (nano)particles (Ni et al., submitted for publication) and that act as a buffering system. It follows that the negatively charged protein/biopolymer layer coating of the Se(0) particles adds to the overall colloidal stability. Chemically-synthesized selenium particles have been shown to precipitate out from solution within minutes provided they are not stabilized with a capping agent (Johnson et al., 2008). In the case of chemogenic non-stabilized (nano)particles, pH is the key element that determines the surface charge and its magnitude (Uhm and Kim, 2014).

4.3. Sediment characterization

The volume of sediment formed is an important factor in a coagulation–flocculation approach. Sediment disposal and residuals management are serious challenges for wastewater treatment plants. Since both coagulants showed a delay in sedimentation for the lower doses employed (Fig. 4a), this suggests the presence of a critical point in colloidal particle destabilization that should be reached in order to induce sedimentation. Beyond this point, the sedimentation depends on the nature and concentration of the coagulant but also on the colloidal particle characteristics (size, shape, surface charge, surface coating). Aluminum sulfate treatment produced three times more sediment than the $FeCl_3$ addition and this was consistent with the higher turbidity removal by the former. Interestingly, the decrease in turbidity removal beyond 2.7×10^{-4} M ferric chloride is not paralleled by a lower sediment volume. A possible explanation could be the composition of the sediments whereby $Fe(OH)_3$ and $Al(OH)_3$ have different contributions. Even if ferric chloride showed a lower efficiency in Se(0) coagulation, $Fe(OH)_3$ precipitates out from the solution and adds to the overall sediment volume.

Dewatering is a challenging task in coagulation–flocculation because less sediment volume means lower transportation and disposal costs. The Capillary Suction Time (CST) describes the tendency of the sediment to lose its water content and therefore reduce its volume (Scholz, 2005). The shorter the CST time (in seconds), the more prone the sediment is to dewatering. The opposite CST results (Fig. 5b) observed in the current study can be linked to the floc structure of each sediment type. Fe-based sediments were shown to exhibit higher CST values and consequently a higher resistance to water removal than aluminum sulfate sediments (Turchiuli and Fargues, 2004). A possible explanation can be the smaller and less compact nature of iron flocs that allow them to retain water more tightly (Turchiuli and Fargues, 2004). Furthermore, the mineralogy and the structure of the sediments can be a key factor. Staicu et al. (2014) showed that Fe–Se sediments produced by electrocoagulation have a reticular structure, whereas Al–Se sediments lack an organized structure. These results can be linked to the lower dewaterability of Fe–Se sediments over their Al–Se counterpart.

The recovery and reuse of materials are important aspects of sustainable development. The resulted Al–Se and Fe–Se sediments could potentially be used as starting materials for Se recovery. Alternatively, since both Fe and Se are essential nutrients, the Fe–Se sediment might be considered as an amendment for Se deficient soils, e.g. in Ireland, India and Finland (Alfthan et al., 2014). Further investigation is required to fully assess the environmental impact of these sediments when applying Fe–Se sediments as potential fertilizers.

4.4. Biogenic Se(0) particle characteristics

Biogenic elemental selenium particles are produced by the metabolically driven reduction of selenium oxyanions (Oremland et al., 2004). Although a mass balance of the batch incubations was not made, the presence of residual Se oxyanions in the batch incubations is unlikely. A previous research using anaerobic granular sludge as inoculum and similar conditions as described in this paper (30 °C, pH = 7, anaerobic) gave an almost complete (97–99%) SeO_4^{2-} removal (Lenz et al., 2008). Moreover, possible intermediates of SeO_4^{2-} reduction (e.g. selenite; organic and inorganic selenides) were not detected in those incubations.

The difference in Se(0) size could be a result of the microbial community composition of the inoculum involved in the conversion of selenate. In addition, it has been shown that during stationary phase, *Shewanella* sp. HN-41 produces Se(0) particles with a normal size distribution (Tam et al., 2010). After 14 d of incubation, the inoculum generated Se(0) particles with a normal size distribution (Fig. 1c). The polydispersity index (≈0.18) suggests that even if the particle size ranges from 50 nm to 250 nm, the mechanism involved in biogenic Se(0) production has an important size control capacity. Considering a scale from 0 to 1, a PDI below 0.1 describes a high homogeneity of the particles, whereas high PDI values suggest a broader size distribution (Gaumet et al., 2008). The difference in Se(0) size could also be explained by the different cellular compartments where the particles are formed. The formation of Se(0) can take place in the cell envelope, reduction mediated by membrane-associated respiratory reductases, or inside the cell when toxic selenium oxyanions pass the outer respiratory barrier (Oremland et al., 2004). Moreover, since the Se(0) particles were produced anaerobically, elemental selenium granules can be stored and used when external electron acceptors become scarce (Herbel et al., 2003).

As a side investigation, the biogenic Se(0) particles were therefore subjected to denaturing gel electrophoresis in an attempt to confirm the presence of proteins attached to their surface (Fig. 1d). The vast amount of protein bands that developed after staining may suggest the presence of a protein corona (Del Pino et al., 2014) and its potential involvement in the colloidal stability of the biogenic Se(0). Since Se(0) particle separation and purification by density gradient centrifugation were not performed, it is likely that some of the protein bands present in the gel image were not tightly associated with the Se(0) particles. Nevertheless, even present in large Se(0) and cell debris aggregates, the proteins add to the general colloidal stability. Similarly to other reports (Dobias et al., 2011; Lenz et al., 2011) focused on the identification of the proteins attached to biogenic Se(0) particles produced by pure cultures, it would be interesting to investigate the nature of

the protein coating issued by mixed microbial cultures present in anaerobic granular sludges in a future study.

5. Conclusions

Biogenic Se(0) is colloidally stable between pH 2–12. The high colloidal stability is a direct consequence of the electrostatic forces associated with the Se(0)-protein coating that prevents aggregation and settling. Filtration, centrifugation and coagulation–flocculation can be employed for effective Se(0) particle sedimentation. Of these, coagulation–flocculation by aluminum sulfate has the best performance in the removal of Se(0)-associated turbidity. The difference in the Se(0) removal efficiency by coagulation–flocculation might be due to several factors, including the hydrolysis products of iron and aluminum, as well as floc size and structure. Charge repression of Se(0) particles showed only limited impact on the neutralization of the particle surface charge, suggesting that other mechanisms are likely to play a major role in Se(0) sedimentation. Due to possible differences in the mineralogical state of the two sediments, Al–Se and Fe–Se sediments display opposite dewatering characteristics. Al–Se sediments show a better dewatering potential that Fe–Se sediments. Highly turbid (800–900 NTU) wastewaters containing colloidal biogenic Se(0) can be effectively treated by coagulation–flocculation using aluminum sulfate.

Acknowledgements

The authors would like to thank the European Commission for providing financial support through the Erasmus Mundus Joint Doctorate Programme ETeCoS^3 (Environmental Technologies for Contaminated Solids, Soils and Sediments) under the grant agreement FPA no. 2010-0009. We thank Fred Kruis and his laboratory staff members from UNESCO-IHE (Delft, NL) for their expert technical assistance. We are indebted to Prof. Elizabeth Pilon-Smits from Colorado State University for Se(0)-protein characterization. A special thanks to Dr. Andrea Wong (Colorado State University) for her technical expertise on Transmission Electron Microscopy.

References

Alfthan, G., Eurola, M., Ekholm, P., Venäläinen, E.R., Root, T., Korkalainen, K., Hartikainen, H., Salminen, P., Hietaniemi, V., Aspila, P., Aro, A., 2014. Effects of nationwide addition of selenium to fertilizers on foods, and animal and human health in Finland: from deficiency to optimal selenium status of the population. J. Trace Elem. Med. Biol. http://dx.doi.org/10.1016/j.jtemb.2014.04.009.

Astratinei, V., van Hullebusch, E.D., Lens, P.N.L., 2006. Bioconversion of selenate in methanogenic anaerobic granular sludge. J. Environ. Qual. 35, 1873–1883.

Awual, M.R., Hasan, M.M., Ihara, T., Yaita, T., 2014. Mesoporous silica based novel conjugate adsorbent for efficient selenium(IV) detection and removal from water. Micropor. Mesopor. Mater. 197, 331–338.

Buchs, B., Evangelou, M.W.H., Winkel, L.H.E., Lenz, M., 2013. Colloidal properties of nanoparticular biogenic selenium govern environmental fate and bioremediation effectiveness. Environ. Sci. Technol. 47 (5), 2401–2407.

Canizares, P., Martinez, F., Jimenez, C., Lobato, J., Rodrigo, M.A., 2007. Coagulation and electrocoagulation of wastes polluted with colloids. Sep. Sci. Technol. 42, 2157–2175.

Chapman, P.M., Adams, W.J., Brooks, M., Delos, C.G., Luoma, S.N., Maher, W.A., Ohlendorf, H.M., Presser, T.S., Shaw, P., 2010. Ecological Assessment of Selenium in the Aquatic Environment. SETAC Press, Pensacola, Florida, USA.

Del Pino, P., Pelaz, B., Zhang, Q., Maffre, P., Nienhaus, G.U., Parak, W.J., 2014. Protein corona formation around nanoparticles – from the past to the future. Mater. Horiz. 1, 301–313.

Dobias, J., Suvorova, E.I., Bernier-Latmani, R., 2011. Role of proteins in controlling selenium nanoparticle size. Nanotechnology 22 (19), 195605.

Duan, J., Gregory, J., 2003. Coagulation by hydrolyzing metal salts. Adv. Colloid Interface 100–102, 475–502.

Dungan, R.S., Frankenberger Jr., W.T., 1999. Microbial transformations of selenium and the bioremediation of seleniferous environments. Bioremed. J. 3 (3), 171–188.

Edwards, G.A., Amirtharajah, A., 1985. Removing color caused by humic acids. J. Am. Water Works Assoc. 77, 50–57.

El Samrani, A.G., Lartiges, B.S., Villieras, F., 2008. Chemical coagulation of combined sewer overflow: heavy metal removal and treatment optimization. Water Res. 42, 951–960.

Fellowes, J.W., Pattrick, R.A.D., Green, D.I., Dent, A., Lloyd, J.R., Pearce, C.I., 2011. Use of biogenic and abiotic elemental selenium nanospheres to sequester elemental mercury released from mercury contaminated museum specimens. J. Hazard. Mater. 189, 660–669.

Gaumet, M., Vargas, A., Gurny, R., Delie, F., 2008. Nanoparticles for drug delivery: the need for precision in reporting particle size parameters. Eur. J. Pharm. Biopharm. 69 (1), 1–9.

Gregory, J., Duan, J., 2001. Hydrolyzing metal salts as coagulants. Pure Appl. Chem. 73 (12), 2017–2026.

Herbel, M.J., Switzer Blum, J., Borglin, S.E., Oremland, R.S., 2003. Reduction of elemental selenium to selenide: experiments with anoxic sediments and bacteria that respire Se-oxyanions. Geomicrobiol. J. 20, 587–602.

Hogg, R., 2005. Flocculation and dewatering of fine-suspension particles. In: Stechemesser, H., Dobias, B. (Eds.), Coagulation and Flocculation, second ed. CRC Press, Florida, USA.

Holt, P.K., Barton, G.W., Wark, M., Mitchell, C.A., 2002. A quantitative comparison between chemical dosing and electrocoagulation. Colloid Surf. A 211, 233–248.

Institute of Medicine (IOM), 2000. Dietary Reference Intakes for Vitamin C, Vitamin E, Selenium, and Carotenoids. The National Academies Press, Washington, DC.

Jarvis, P., Jefferson, B., Gregory, J., Parsons, S.A., 2005. A review of floc strength and breakage. Water Res. 39 (14), 3121–3137.

Johnson, N.C., Manchester, S., Sarin, L., Gao, Y., Kulaots, I., Hurt, R.H., 2008. Mercury vapor release from broken compact fluorescent lamps and in situ capture by new nanomaterial sorbents. Environ. Sci. Technol. 42 (15), 5772–5778.

Johnson, A.C., Jürgens, M.D., Lawlor, A.J., Cisowska, I., Williams, R.J., 2014. Particulate and colloidal silver in sewage effluent and sludge discharged from British wastewater treatment plants. Chemosphere 112, 49–55.

Jung, A.V., Chanudet, V., Ghanbaja, J., Lartiges, B.S., Bersillon, J.L., 2005. Coagulation of humic substances and dissolved organic matter with a ferric salt: an electron energy loss spectroscopy investigation. Water Res. 39 (16), 3849–3862.

Kijjanapanich, P., Annachhatre, A.P., Esposito, G., van Hullebusch, E.D., Lens, P.N.L., 2013. Biological sulfate removal from gypsum contaminated construction and demolition debris. J. Environ. Manage. 269, 38–44.

Laemmli, U.K., 1970. Cleavage of structural proteins during the assembly of the head of bacteriophage T4. Nature 227, 680–685.

Lemly, A.D., 2004. Aquatic selenium pollution is a global environmental safety issue. Ecotox. Environ. Saf. 59, 44–56.

Lenz, M., Lens, P.N.L., 2009. The essential toxin: the changing perception of selenium in environmental sciences. Sci. Total Environ. 407, 3620–3633.

Lenz, M., van Hullebusch, E.D., Hommes, G., Corvini, P.F.X., Lens, P.N.L., 2008. Selenate removal in methanogenic and sulfate-reducing upflow anaerobic sludge bed reactors. Water Res. 42, 2184–2194.

Lenz, M., Kolvenbach, B., Gygax, B., Moes, S., Corvinni, P.F.X., 2011. Shedding light on selenium biomineralization: proteins associated with bionanominerals. Appl. Environ. Microbiol. 77 (13), 4676–4680.

Levander, O.A., Burk, R.F., 2006. Update of human dietary standards for selenium. In: Hatfield, D.L., Berry, M.J., Gladyshev, V.N. (Eds.), Selenium – Its Molecular Biology and Role in Human Health. Springer, New York, USA.

Li, H., Zhang, J., Wang, T., Luo, W., Zhou, Q., Jiang, G., 2008. Elemental selenium particles at nano-size (Nano-Se) are more toxic to Medaka (*Oryzias latipes*) as a consequence of hyper-accumulation of selenium: a comparison with sodium selenite. Aquat. Toxicol. 89 (4), 251–256.

Luoma, S.N., Johns, C., Fisher, N.S., Steinberg, N.A., Oremland, R.S., Reinfelder, J.R., 1992. Determination of selenium bioavailability to a bivalve from particulate and solute pathways. Environ. Sci. Technol. 26, 485–491.

Martin, R.B., 1991. Fe^{3+} and Al^{3+} hydrolysis equilibria. Cooperativity in Al^{3+} hydrolysis reactions. J. Inorg. Biochem. 44 (2), 141–147.

Ni, T.W., Staicu, L.C., Schwartz, C., Crawford, D., Nemeth, R., Seligman, J., Hunter, W.J., Pilon-Smits, E.A.H., Ackerson, C.J., submitted for publication. Progress toward clonable inorganic particles. ACS Nano (2014).

Oremland, R.S., Herbel, M.J., Blum, J.S., Langley, S., Beveridge, T.J., Ajayan, P.M., Sutto, T., Ellis, A.V., Curran, S., 2004. Structural and spectral features of selenium nanospheres produced by Se-respiring bacteria. Appl. Environ. Microbiol. 70 (1), 52–60.

Richens, D.T., 1997. The Chemistry of Aqua Ions. Wiley, Chichester, UK.

Russel, W.B., Saville, D.A., Schowalter, W.R., 1992. Colloidal Dispersions. Cambridge University Press, UK.

Schlekat, C.E., Dowdle, P.R., Lee, B.G., Luoma, S.N., Oremland, R.S., 2000. Bioavailability of particle-associated selenium on the bivalve *Potamocorbila amuresis*. Environ. Sci. Technol. 34, 4504–4510.

Scholz, M., 2005. Review of recent trends in Capillary Suction Time (CST) dewaterability testing research. Ind. Eng. Chem. Res. 44 (22), 8157–8163.

Scholz, M., 2006. Revised capillary suction time (CST) test to reduce consumable costs and improve dewaterability interpretation. J. Chem. Technol. Biotechnol. 81, 336–344.

Simmons, D.B., Wallschlaeger, D., 2005. A critical review of the biogeochemistry and ecotoxicology of selenium in lotic and lentic environments. Environ. Toxicol. Chem. 24 (6), 1331–1343.

Sobolewski, A., 2013. Evaluation of Treatment Options to Reduce Water-borne Selenium at Coal Mines in West-Central Alberta. Microbial Technologies, Inc. <http://environment.gov.ab.ca/info/library/7766.pdf>.

Staicu, L.C., van Hullebusch, E.D., Lens, P.N.L., Pilon-Smits, E.A.H., Oturan, M.A., 2014. Electrocoagulation of colloidal biogenic selenium. Environ. Sci. Pollut. Res. http://dx.doi.org/10.1007/s11356-014-3592-2.

Stams, A.J.M., van Dijk, J.B., Dijkema, C., Plugge, C.M., 1993. Growth of syntrophic propionate-oxidizing bacteria with fumarate in the absence of methanogenic bacteria. Appl. Environ. Microbiol. 59, 1114–1119.

Tam, K., Ho, C.T., Lee, J.H., Lai, M., Chang, C.H., Rheem, Y., Chen, W., Hur, H.G., Myung, N.V., 2010. Growth mechanism of amorphous selenium nanoparticles synthesized by *Shewanella* sp. HN-41. Biosci. Biotechnol. Biochem. 74 (4), 696–700.

Tambo, N., 1991. Basic concepts and innovative turn of coagulation/flocculation. Water Supp. 9, 1–10.

Thuvander, J., Arkell, A., Jönsson, A.-S., 2014. Centrifugation as pretreatment before ultrafiltration of hemicelluloses extracted from wheat bran. Sep. Purif. Technol. 138, 1–6.

Tinggi, U., 2003. Essentiality and toxicity of selenium and its status in Australia: a review. Toxicol. Lett. 137 (1–2), 103–110.

Turchiuli, C., Fargues, C., 2004. Influence of structural properties of alum and ferric flocs on sludge dewaterability. Chem. Eng. J. 103 (1–3), 123–131.

Uhm, H.N., Kim, Y., 2014. Sensitivity of nanoparticles' stability at the point of zero charge (PZC). J. Ind. Eng. Chem. 20 (5), 3175–3178.

USEPA, 1999. Enhanced coagulation and enhanced precipitative softening guidance manual. EPA 815-R-99-012.

Wen, H., Carignan, J., 2007. Reviews on atmospheric selenium: emissions, speciation and fate. Atmos. Environ. 41, 7151–7165.

Yang, G., Yin, S., Zhou, R., Gu, L., Yan, B., Liu, Y., Liu, Y.J., 1989. Studies of safe maximal daily dietary Se-intake in a seleniferous area in China. Part II: Relation between Se-intake and the manifestation of clinical signs and certain biochemical alterations in blood and urine. Trace Elem. Electrolytes Health Dis. 3, 123–130.

Zhang, Y., Zahir, Z.A., Frankenberger Jr., W.T., 2004. Fate of colloidal-particulate elemental selenium in aquatic systems. J. Environ. Qual. 33, 559–564.

Zhang, E.S., Wang, H.L., Yan, X.X., Zhang, L.D., 2005. Comparison of short-term toxicity between Nano-Se and selenite in mice. Life Sci. 76, 1099–1109.

Zhao, Y.X., Gao, B.Y., Shon, H.K., Cao, B.C., Kim, J.H., 2011. Coagulation characteristics of titanium (Ti) salt coagulant compared with aluminum (Al) and iron (Fe) salts. J. Hazard. Mater. 185, 1536–1542.